Low pH, Aluminum, and Phosphorus Coordinately Regulate Malate Exudation through *GmALMT1* to Improve Soybean Adaptation to Acid Soils[1][W][OA]

Cuiyue Liang, Miguel A. Piñeros, Jiang Tian, Zhufang Yao, Lili Sun, Jiping Liu, Jon Shaff, Alison Coluccio, Leon V. Kochian, and Hong Liao*

State Key Laboratory for Conservation and Utilization of Subtropical Agro-Bioresources, Root Biology Center, South China Agricultural University, Guangzhou 510642, People's Republic of China (C.L., J.T., Z.Y., L.S., H.L.); Robert W. Holley Center for Agriculture and Health, United States Department of Agriculture-Agricultural Research Service, Cornell University, Ithaca, New York 14853 (C.L., M.A.P., J.L., J.S., A.C., L.V.K.); and Institute of Tropical Crop Genetic Resources, Chinese Academy of Tropical Agriculture Sciences, Danzhou 571737, People's Republic of China (L.S.)

Low pH, aluminum (Al) toxicity, and low phosphorus (P) often coexist and are heterogeneously distributed in acid soils. To date, the underlying mechanisms of crop adaptation to these multiple factors on acid soils remain poorly understood. In this study, we found that P addition to acid soils could stimulate Al tolerance, especially for the P-efficient genotype HN89. Subsequent hydroponic studies demonstrated that solution pH, Al, and P levels coordinately altered soybean (*Glycine max*) root growth and malate exudation. Interestingly, HN89 released more malate under conditions mimicking acid soils (low pH, +P, and +Al), suggesting that root malate exudation might be critical for soybean adaptation to both Al toxicity and P deficiency on acid soils. *GmALMT1*, a soybean malate transporter gene, was cloned from the Al-treated root tips of HN89. Like root malate exudation, *GmALMT1* expression was also pH dependent, being suppressed by low pH but enhanced by Al plus P addition in roots of HN89. Quantitative real-time PCR, transient expression of a GmALMT1-yellow fluorescent protein chimera in Arabidopsis protoplasts, and electrophysiological analysis of *Xenopus laevis* oocytes expressing GmALMT1 demonstrated that *GmALMT1* encodes a root cell plasma membrane transporter that mediates malate efflux in an extracellular pH-dependent and Al-independent manner. Overexpression of *GmALMT1* in transgenic Arabidopsis, as well as overexpression and knockdown of *GmALMT1* in transgenic soybean hairy roots, indicated that GmALMT1-mediated root malate efflux does underlie soybean Al tolerance. Taken together, our results suggest that malate exudation is an important component of soybean adaptation to acid soils and is coordinately regulated by three factors, pH, Al, and P, through the regulation of *GmALMT1* expression and GmALMT1 function.

Up to one-half of the world's potentially arable lands are composed of acid soils, which limit crop productivity in these regions (von Uexküll and Mutert, 1995). The stresses imposed on crops growing on acid soils consist of proton rhizotoxicity (low pH), nutrient deficiency (primarily phosphorus [P] but also potassium, calcium, and other minerals), and metal toxicity (aluminum [Al] and manganese). Among these constraints, low P availability, toxic levels of Al, and proton rhizotoxicity (low-pH stress) are considered to be the three major stresses limiting plant growth on acid soils (Kochian et al., 2004).

The harmful effects of low pH for plants growing on acid soils can be direct or indirect. Low pH can directly inhibit root growth (Wilkinson and Duncan, 1989; Schubert et al., 1990; Kinraide, 1998, 2003; Koyama et al., 2001; Yang et al., 2005). Calcium may ameliorate the inhibition of root growth by low pH through stabilizing the pectic polysaccharide network in the cell wall (Koyama et al., 2001). Change in organic acid metabolism is another putative mechanism for plant adaptation to low-pH stress, possibly via a cytoplasmic pH "stat" mechanism, as was suggested in a study of the response of isolated wheat (*Triticum aestivum*) aleurone layers to low pH (Martínez-Camacho et al., 2004). Recently, the expression of the malate transporter gene that underlies Arabidopsis (*Arabidopsis thaliana*) Al tolerance, *AtALMT1*, was found to be regulated in part by the transcription factor *STOP1*, which was identified via map-based cloning of an Arabidopsis mutant hypersensitive to low-pH stress (Iuchi et al., 2007; Sawaki et al., 2009).

[1] This work was supported by the National Key Basic Research Special Funds of China (grant no. 2011CB100301) and the National Natural Science Foundation of China (grant no. 31025022).

* Corresponding author; e-mail hliao@scau.edu.cn.

The author responsible for distribution of materials integral to the findings presented in this article in accordance with the policy described in the Instructions for Authors (www.plantphysiol.org) is: Hong Liao (hliao@scau.edu.cn).

[W] The online version of this article contains Web-only data.

[OA] Open Access articles can be viewed online without a subscription.

www.plantphysiol.org/cgi/doi/10.1104/pp.112.208934

In acid soils, toxic forms of Al are released when the pH drops to 5 or lower. These active Al species, primarily Al^{3+}, can cause root damage and root growth inhibition by targeting the cell wall (Horst et al., 1999), the cytoskeleton (Sivaguru et al., 1999), callose production (Sivaguru et al., 2000), DNA (Yamaguchi et al., 1999; Meriga et al., 2004), and the plasma membrane (Elstner et al., 1988) and disturbing stress-signaling pathways including the regulation of cytosolic free Ca^{2+} activities (Ramos-Díaz et al., 2007). Consequently, the inhibition of root growth and function on acid soils results in the severe impairment of water and nutrient acquisition by roots, leading to a significant reduction in crop yields (Ryan et al., 2001; Kochian et al., 2004). Over the past few decades, significant progress has been made in understanding the physiological and molecular mechanisms underlying Al tolerance in plants (Archambault et al., 1997; Degenhardt et al., 1998; Basu et al., 1999; Ma, 2000; Sasaki et al., 2004; Huang et al., 2009, 2010; Yamaji et al., 2009). Al-activated root malate efflux is considered to be one of the major mechanisms for Al tolerance in a number of plant species, including wheat, Arabidopsis, and triticale (*Triticum* × *Secale* hexaploid; Delhaize et al., 1993b; Pellet et al., 1996; Larsen et al., 1998; Ma et al., 2000). Seminal work in this area came from Sasaki et al. (2004), who identified the *TaALMT1* (for Al-activated malate transporter) gene, which encodes a membrane transporter mediating Al-activated root malate efflux in wheat root tips. Since that first study, *ALMT* genes involved in Al tolerance have been cloned and characterized in Arabidopsis (Hoekenga et al., 2006) and rape (*Brassica napus*; Ligaba et al., 2006). It has been shown that overexpression of *ALMT* genes not only enhanced malate exudation but also improved Al tolerance in transgenic plants (Delhaize et al., 2009).

P deficiency is another major soil constraint to agricultural production, limiting crop yield in 30% to 40% of the arable lands in the world (Runge-Metzger, 1995). Plants have evolved a series of adaptive strategies, such as the exudation of organic acids, in order to adapt to P deficiency in soils. Secreted organic anions mobilize P either by anion exchange or chelating metal ions that form immobile complexes with P in the soil (Lipton et al., 1987; Vance et al., 2003). Plant species such as white lupin (*Lupinus albus*), buckwheat (*Fagopyrum esculentum*), and rape are quite efficient in mobilizing phosphate (Pi) from inorganic P complexes in the soil through enhanced malate exudation from roots (Hoffland et al., 1989; Hinsinger, 2001; Sas et al., 2001).

Since P deficiency and Al toxicity usually coexist in acid soils (Kochian et al., 2004), the effects of P-Al interactions on plant adaptation to Al toxicity have been studied (Dong et al., 2004; Zheng et al., 2005; Liao et al., 2006; Jemo et al., 2007; Sun et al., 2008). Fukuda et al. (2007) suggested that a common metabolic system is responsive to both P deficiency and Al toxicity in rice. Tan and Keltjens (1990a, 1990b) showed that P could ameliorate Al toxicity by improving root development and nutrient uptake in sorghum (*Sorghum bicolor*). Moreover, it has been suggested that immobilization of Al by P in the root cell wall is a potential mechanism for Al tolerance in buckwheat (Zheng et al., 2005), barley (*Hordeum vulgare*; McCormick and Borden, 1972), and maize (*Zea mays*; Gaume et al., 2001). Recently, organic acid exudation has been suggested to be involved in the P-dependent Al tolerance in plants. Ligaba et al. (2004) showed that the P-sufficient rape accumulated and secreted more Al-activated organic anions than the P-deficient plants. In our previous study, under Al stress in hydroponics, P application to shallow lateral roots in a divided root system was shown to stimulate malate exudation from the tap root tip of the P-efficient soybean (*Glycine max*) genotypes compared with the P-inefficient genotypes, which also correlated with superior Al tolerance (Liao et al., 2006).

Although the mechanistic basis for P and Al interactions has been taken into consideration in a few studies on plant adaptation to acid soils, this subject is still quite poorly understood, and the integration of H^+ and Al toxicity with P availability has not been addressed. Plants might adapt to low-pH stress and Al toxicity through the same biological processes, as suggested by the identification of common H^+- and Al-responsive genes in an Arabidopsis microarray analysis (Sawaki et al., 2009).

In this study, we first conducted a field trial to elucidate the responses of soybean growth of a P-efficient and a P-inefficient cultivar to heterogeneously distributed low pH, high Al, and low P in acid soils. Subsequently, hydroponic experiments were carried out to analyze the coordinated regulation of root growth and root malate exudation by low pH, Al toxicity, and differential P availability. Furthermore, a soybean homolog of the wheat *ALMT1*, *GmALMT1*, was isolated and characterized. The transcriptional regulation of *GmALMT1* by low pH, Al toxicity, and P availability was investigated. Transient expression of a GmALMT1-YFP (for yellow fluorescent protein) chimera in Arabidopsis protoplasts and electrophysiological analysis in *Xenopus laevis* oocytes expressing GmALMT1 demonstrated that *GmALMT1* encodes a plasma membrane malate transporter. The in planta role of GmALMT1 in root malate exudation and Al tolerance was demonstrated via overexpression in transgenic Arabidopsis plants as well as overexpression and knockdown of *GmALMT1* in transgenic soybean hairy roots.

RESULTS

Performance of Soybean in Acid Soils at Two P Levels

Soil pH, Al, and P contents were found to be heterogeneously distributed along vertical acid soil profiles in the field; thus, these acid soils could be divided into three layers (Supplemental Table S1). With increasing soil depth, the pH value and exchangeable P content significantly decreased, whereas the exchangeable Al content significantly increased. In the

deepest soil layer (40–60 cm), exchangeable P was totally undetectable and the pH value had decreased to 4.29 (from pH 5.71 in the 0- to 20-cm soil layer), while the exchangeable Al content increased to 3.04 centimoles kg^{-1}, which was twice that measured in the top soil layer (0–20 cm).

A previous study from our laboratory showed that HN89 is a P-efficient genotype, while HN112 is a P-inefficient genotype (Zhao et al., 2004). The growth performance of these two soybean genotypes was investigated on acid soils at two P levels (Fig. 1). Without P application, total root lengths of HN89 (a P-efficient genotype) and HN112 (a P-inefficient genotype) were almost identical. P fertilization to the topsoil resulted in a significant increase (about 42%) in total root length for the P-efficient genotype (HN89) in response to P application (Fig. 1A). In contrast, the total root length in the P-inefficient genotype HN112 was relatively unaffected. Furthermore, total plant biomass was significantly higher in the P-efficient genotype HN89 relative to that of the P-inefficient genotype HN112 at both P levels (Fig. 1B). Plant dry weight of HN89 was 100% and 75% greater than that of HN112 at low and high P levels, respectively. These findings suggested that the enhanced growth of the P-efficient genotype upon supplying P might partially result from enhanced Al tolerance via improved root growth. This possibility was investigated further as detailed below.

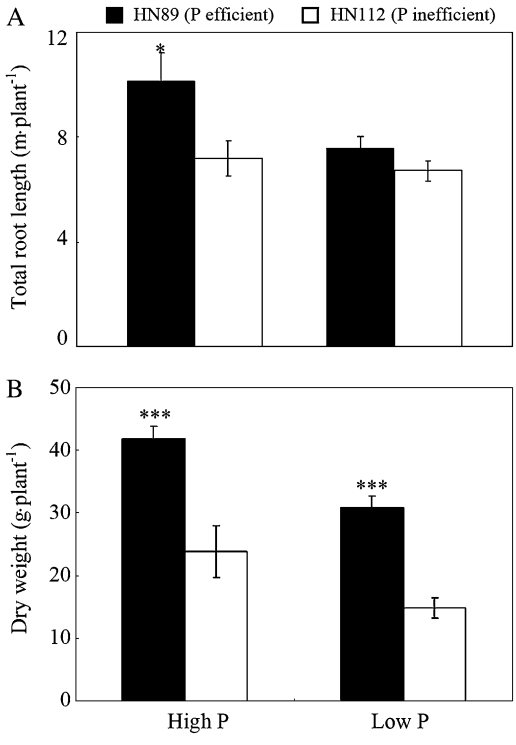

Figure 1. Total root length (A) and total plant dry weight (B) for the P-efficient (HN89) and P-inefficient (HN112) soybean genotypes grown on acid soils with two different P applications. Plants were grown on acid soils under low-P (no P added) and high-P (80 kg P_2O_5 ha^{-1} added as triple superphosphate) conditions for 60 d. Each bar represents the mean of six replicates ± SE. Asterisks indicate significant differences between the two genotypes in the same treatment: $*P < 0.05$, $***P < 0.001$.

Interaction of Al, pH, and P on Soybean Root Growth

To elucidate plant responses to the interactions among Al, low pH, and P, relative root growth was quantified in soybean plants grown in hydroponic culture under specific pH, Al, and P conditions. The results showed that Al tolerance was influenced by P availability (Fig. 2). Under low-P conditions, the relative root growth of both soybean genotypes was significantly inhibited by Al addition (52% and 49% inhibition in HN89 and HN112, respectively). Under +P conditions, the adverse effects of Al on relative root growth were ameliorated in both genotypes (Fig. 2), with the P-efficient genotype HN89 exhibiting a significantly higher relative root growth than HN112 under this treatment (115% versus 90%). These results were consistent with the results from the field studies (Fig. 1A), indicating that the P-efficient genotype HN89 was more Al tolerant, but only under conditions of P supply. However, the two genotypes showed no significant differences in relative root growth in response to low pH or P availability under –Al conditions (Fig. 2).

Changes in Root Malate Content and Exudation in Response to pH, P, and Al

Root malate exudation and internal malate content of soybean root tips were found to be coordinately influenced by changes in pH, P, and Al in the growth medium (Fig. 3). In the higher pH nutrient solution (pH 5.8), malate exudation in the P-efficient genotype HN89 was significantly higher than in the P-inefficient genotype HN112, independent of the P treatment (Fig. 3A). Acidification (pH 4.3) of the nutrient solution resulted in a significant reduction in root malate exudation (70% and 55% in HN89 and HN112, respectively) under high-P supply. Addition of Al to this high-P/low-pH nutrient solution increased malate exudation by 130% and 43% in NH89 and NH112, respectively. In contrast, the effects of medium acidification and the addition of Al were less pronounced under low-P supply. Interestingly, under conditions mimicking acid soils (low pH, +P, and +Al), roots of the P-efficient genotype HN89 secreted more malate than those from the P-inefficient genotype HN112 (Fig. 3A). This result suggests that the role of root malate exudation is more than just a response to toxic Al in soybean roots on acid soils, such that the enhanced malate exudation at low pH and low P availability might also be involved in the plant-mediated release of Pi from insoluble P forms on acid soils.

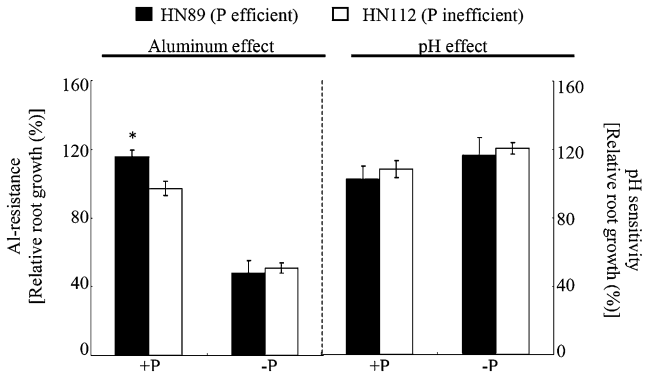

Figure 2. Root growth was influenced by pH, Al, and P in both soybean genotypes. Al resistance was based on relative root growth calculated as the root growth under +Al conditions relative to the root growth under –Al conditions. Low-pH-based relative root growth was calculated as the root growth for plants grown on nutrient solution at pH 4.3 relative to the root growth of plants grown in nutrient solution at pH 5.8. P treatments (–P and +P) represent application of 0 and 320 μM KH_2PO_4, respectively; −Al and +Al indicate application of 0 and 38 μM Al^{3+} activity, respectively. Each value is the mean of four replicates ± SE. The asterisk indicates a significant difference between the two genotypes in the same treatment: $*P < 0.05$.

Although the internal malate content in root tips from both genotypes also decreased significantly upon acidification on the growth medium, root malate content was not affected by Al treatment (Fig. 3B). Furthermore, in contrast to the changes in malate exudation observed under high-P and +Al/−Al, the addition of P in the low-pH solution resulted in an Al-independent and moderate increase in malate content in the root tips of both genotypes. Interestingly, the P-efficient genotype HN89 maintained significantly higher root tip malate content than did the P-inefficient genotype HN112 throughout most treatments (except high P and pH). Overall, these findings suggest that the maintenance of malate synthesis/accumulation in root tips is significantly influenced by external pH and the P efficiency of plants.

Isolation of the Malate Transporter Gene, *GmALMT1*, from Soybean

A 405-bp *GmALMT1* fragment was amplified from complementary DNA (cDNA) derived from soybean root tips of HN89 subjected to Al treatment using a pair of degenerate primers based on the conserved sequence motif from the Al-dependent malate transporters TaALMT1 (Sasaki et al., 2004), AtALMT1 (Hoekenga et al., 2006), and BnALMT1 (Ligaba et al., 2006). This fragment was used to obtain the corresponding full-length cDNA via RACE-PCR. The coding region of *GmALMT1* (National Center for Biotechnology Information GenBank accession no. ACC60273) was 1,461 bp in length, with the deduced protein consisting of 486 amino acid residues. BLAST analysis indicated that GmALMT1 was 46% identical to AtALMT1 from Arabidopsis, 48% identical to BnALMT1 from rape, and 43% identical to TaALMT1 from wheat.

Phylogenetic analysis showed that soybean ALMT family member proteins and ALMTs with known functions in other plants species could be grouped into three clades (Supplemental Fig. S1). AtALMT9 and AtALMT12 were grouped into clade I and clade II, respectively, while other ALMT1 proteins together with GmALMT1 were grouped into clade III. Interestingly, those ALMTs in clade III were further classified into two subgroups, the monocot group (i.e. ZmALMT1, TaALMT1, and HvALMT1) and the dicot group (i.e. GmALMT1, BnALMT1, BnALMT2, and AtALMT1; Supplemental Fig. S1).

GmALMT1 Expression Is Regulated by pH and Al

Quantitative real-time PCR (qRT-PCR) was used to analyze *GmALMT1* expression patterns in soybean seedlings. As shown in Figure 4A, *GmALMT1* expression was primarily localized to the root apex of tap roots (Fig. 4A). In the absence of Al stress, a low expression level of *GmALMT1* was observed in the root tips (first 0–2 cm of the root), being almost undetectable in the other root regions. However, after 6 h of Al^{3+} exposure, the level of *GmALMT1* transcript abundance was increased by more than 3-fold in the root

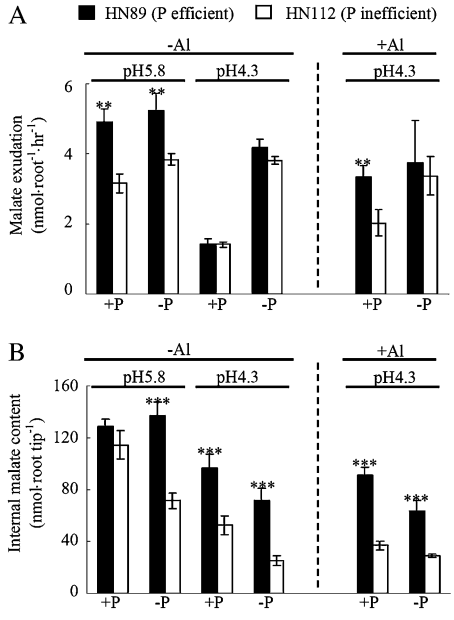

Figure 3. Root malate exudation (A) and malate content in root tips (B) as influenced by pH, Al, and P in both soybean genotypes. −P and +P represent application of 0 and 320 μM KH_2PO_4, respectively; the pH treatments are pH 4.3 and 5.8; −Al and +Al indicate application of 0 and 38 μM Al^{3+} activity, respectively. Each data point is the mean of four replicates ± SE. Asterisks indicate significant differences between the two genotypes in the same treatment. $**0.001 < P < 0.01$, $***P < 0.001$.

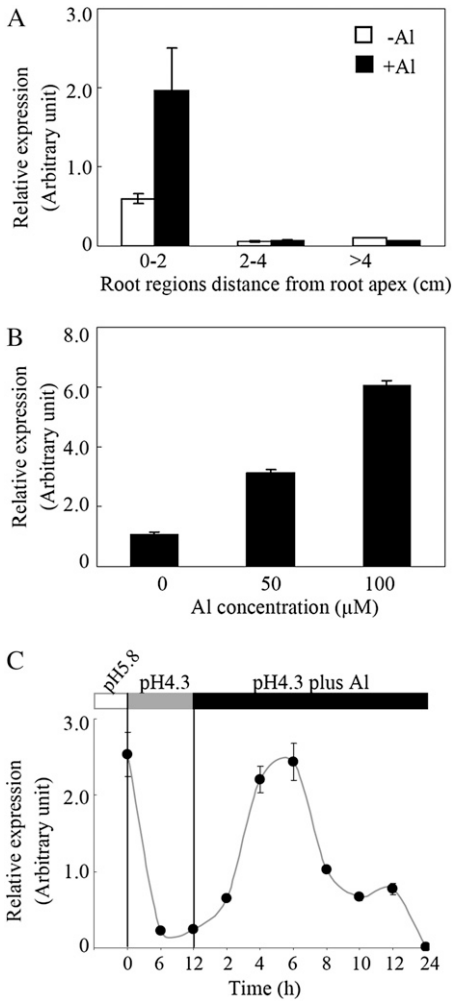

Figure 4. Expression patterns of *GmALMT1* in response to low pH and Al toxicity. A, Spatial expression pattern of *GmALMT1* in soybean tap roots with or without 50 μM $AlCl_3$. B, Al dose response of *GmALMT1* in root tips (0–2 cm). Seedlings were separately treated with 0, 50, and 100 μM $AlCl_3$ for 6 h. C, Temporal expression pattern of *GmALMT1* in root tips (0–2 cm) in response to a pH shift from 5.8 to 4.3, followed by the addition of Al. Seedlings were subjected to low pH (4.3) for 12 h and subsequently transferred to the same solution containing 50 μM $AlCl_3$ for up to 24 h. Each data point is the mean of four replicates ± SE.

tips, while no significant changes of *GmALMT1* expression were observed in the other root regions (Fig. 4A). Expression of *GmALMT1* in the root tip was Al dependent, increasing with increasing Al levels (Fig. 4B). To determine whether *GmALMT1* expression was affected by the interaction of pH and Al toxicity, temporal expression patterns of *GmALMT1* were also examined in the root tips. As shown in Figure 4C, the expression of *GmALMT1* in the root tips was regulated both by pH and Al. The levels of *GmALMT1* expression were high in the root tips of the seedlings grown in pH 5.8 nutrient solution prior to subjecting the seedling roots to low pH (Fig. 4C). The *GmALMT1* expression decreased by more than 12-fold after 6 h of low-pH treatment, remaining low over the next 6 h. Inclusion of Al in the low-pH solution resulted in a 2-fold increase of *GmALMT1* transcript abundance within 2 h of Al exposure, increasing up to 4- to 5-fold after 4 to 6 h of Al treatment. Thereafter, expression levels of *GmALMT1* gradually decreased over the next 18 h of Al treatment (Fig. 4C). These results indicated that low pH strongly suppressed, while Al^{3+} transiently enhanced, the expression of *GmALMT1*, with the enhancement of *GmALMT1* expression by Al^{3+} being greater than the suppression by low pH.

GmALMT1 Expression Appears to Be Coordinately Regulated by P, pH, and Al

As shown in Figure 5, the expression levels of *GmALMT1* in soybean roots appeared to be coordinately regulated by pH, Al, and P. The levels of *GmALMT1* transcript abundance in both genotypes decreased at low pH, with this response being partly dependent on P availability (Fig. 5). In +P conditions, *GmALMT1* expression under the higher pH conditions (pH 5.8) was approximately 3-fold higher than that measured under low-pH conditions (pH 4.3), with no significant differences observed between genotypes. However, in −P medium at pH 5.8, *GmALMT1* expression in the P-efficient genotype HN89 was significantly higher than in HN112 (P inefficient). When the −P growth solution pH was decreased to pH 4.3, there were only 20% and 40% decreases in *GmALMT1* transcript abundance in HN89 and HN112, respectively, which were significantly smaller low-pH-induced decreases in expression compared with the reductions observed in the +P medium (Fig. 5). These findings are in agreement with the root malate exudation data shown in Figure 3A, where lowering the

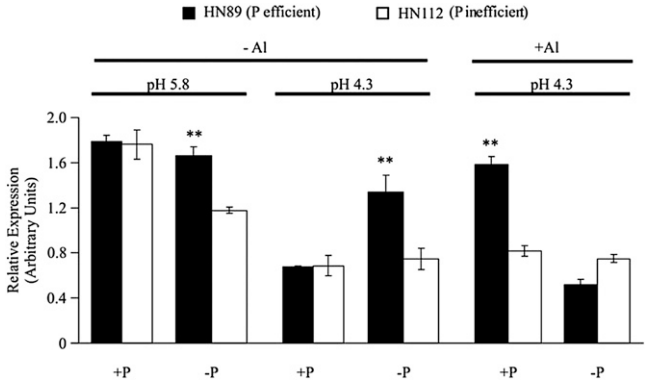

Figure 5. *GmALMT1* expression in root tips (0–2 cm) appears to be coordinately regulated by pH, Al, and P. −P and +P represent application of 0 and 320 μM KH_2PO_4, respectively; the pH treatments are pH 4.3 and 5.8; −Al and +Al indicate application of 0 and 38 μM Al^{3+} activity, respectively. Al treatments were performed for 6 h. Each data point is the mean of four replicates ± SE. Asterisks indicate significant differences between the two genotypes in the same treatment: $^{**}0.001 < P < 0.01$.

pH in the +P growth solution resulted in a significant decrease in root malate exudation in both genotypes, consistent with the reduction in *GmALMT1* expression levels seen in Figure 5. Further regression statistical analysis showed that the coefficiency (r^2) between malate exudation and *GmALMT1* expression was 0.83 or 0.71 at high or low P, respectively, which was significant at 0.05, suggesting that malate exudation is highly regulated by *GmALMT1* expression. Likewise, and most relevant to the coordinate regulation of Al tolerance, inclusion of Al in the pH 4.3 treatment solution resulted in a significant increase in root malate exudation predominantly in the P-efficient genotype HN89 (Fig. 3A), and the same treatment resulted in a significant increase in *GmALMT1* expression only in the P-efficient genotype HN89, and only in response to +P treatment.

GmALMT1 Is a Plasma Membrane-Localized Transport Protein

Like other plant ALMTs, the GmALMT1 protein is predicted to harbor six membrane-spanning domains in the protein using hydropathy plot analysis (TMHMM Server; http://www.cbs.dtu.dk/services/TMHMM-2.0/). The cellular localization of GmALMT1 was investigated by transiently expressing the YFP::GmALMT1 translational fusion in Arabidopsis leaf protoplasts (Fig. 6). In control protoplasts (transformed with the empty vector), fluorescence associated with the soluble YFP was observed throughout the cytosol. In contrast, in protoplasts transformed with YFP::GmALMT1, the fluorescence was localized predominantly to the cell periphery, suggesting a plasma membrane localization. This was confirmed by the colocalization of the fluorescence from the YFP::GmALMT1 protein with the fluorescence associated with the plasma membrane-specific fluorescent dye (Fig. 6, right column).

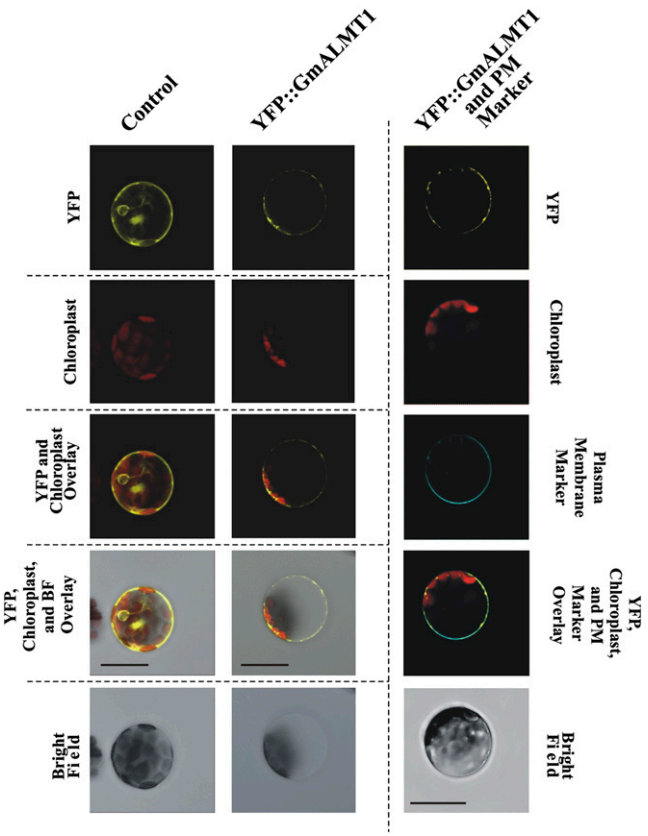

Figure 6. Cellular localization of the GmALMT1 protein in Arabidopsis protoplasts. The left and middle columns show representatives cells transformed with pSAT6-EYFP-C1 empty vector (as a control) and YFP::GmALMT1, respectively. Rows showing YFP fluorescence, chloroplast autofluorescence, bright-field images, as well as overlays are as indicated on the left margin. The right column shows representative images of YFP::GmALMT1-transformed cells where the plasma membrane has been stained with CellMask (third row; visible as blue fluorescence). All images are representative of three independent experiments in which 15 or more protoplasts were imaged. Bars = 20 μm.

GmALMT1 Encodes a Membrane Transporter That Mediates Malate Efflux

Functional characterization of GmALMT1 was carried out by heterologously expressing the gene in *X. laevis* cells and examining their electrophysiological properties. Oocytes injected with GmALMT1 complementary RNA (cRNA) had significantly lower negative resting membrane potentials than control cells in standard solutions at both pH 7.5 and 4.5 (Fig. 7A), suggesting that the expression of *GmALMT1* resulted in a reduction of the net internal negative charge (relative to that found in control cells) as a result of net anion influx or net cation efflux. Further characterization was performed using the conventional two-electrode voltage-clamp method (Fig. 7, B and C). In standard bath solutions at pH 7.5, GmALMT1-expressing cells mediated large inward (i.e. negative) currents and smaller outward (i.e. positive) currents. Acidification of the bath medium to pH 4.5 resulted in enhancement of the GmALMT1-mediated outward currents while having no major effect on the GmALMT1-mediated inward currents. In contrast, under both sets of ionic conditions, control cells showed no significant currents within the range of holding potentials tested. Since, by convention, GmALMT1-mediated inward currents are the product of either net positive charge influx or net negative charge efflux (which would be consistent with efflux of the malate anion), to further characterize the nature of the GmALMT1-mediated transport, the intracellular malate activities ($\{mal^{2-}\}_i$) were increased from basal endogenous levels (zero) up to 4.5 mM via microinjection of malate using well-characterized protocols (Piñeros et al., 2008a), thereby increasing the organic anion efflux driving force. Increasing $\{mal^{2-}\}_i$ resulted in a concentration-dependent increase in the GmALMT1-mediated inward currents in standard bath solutions at both pH 7.5 and 4.5 (Fig. 8). In contrast, although being pH

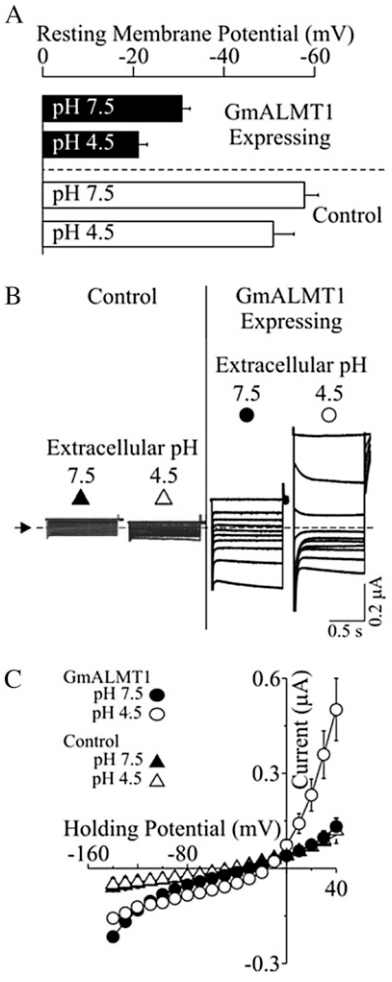

Figure 7. Functional characterization of GmALMT1 expressed in *X. laevis* oocytes. A, Resting membrane potentials of GmALMT1-expressing and control cells measured in standard bath solution at pH 7.5 and 4.5. B, Example of GmALMT1-mediated currents (right panels) elicited in response to holding potentials ranging from +40 to −140 mV (in 20-mV increments) in standard bath solution at pH 7.5 and 4.5. The voltage was held at +40 mV for 10 s between voltage pulses. Currents recorded in control cells (i.e. not injected with cRNA) are shown for reference at left. The dotted line and arrow on the left margin indicate the zero-current level. C, Mean current-voltage curves constructed from the steady-state current recordings such as those shown in B for holding potentials ranging from +40 to −140 mV in 10-mV steps. The symbols correspond to those depicted above the example traces in B.

dependent (i.e. stimulated at lower pH, as shown in Fig. 7), GmALMT1-mediated outward currents were independent of changes in $\{mal^{2-}\}_i$. Under increased $\{mal^{2-}\}_i$ conditions, we were also able to establish that acidification of the bath medium resulted in inhibition of the GmALMT1-mediated inward (i.e. negative) currents at all $\{mal^{2-}\}_i$ tested. Analysis of the slope of GmALMT1-mediated inward current (conductance) at pH 7.5 and 4.5 showed that the inward conductance tended to saturate as the $\{mal^{2-}\}_i$ approached 4 mM, suggesting that the GmALMT1-mediated malate transport saturates with a K_m of about 1 to 2 mM internal malate activities, independent of the extracellular pH value (Fig. 8C). These findings also suggest that decreasing the pH of the bath solution from pH 7.5 to 4.5 results in a change in the maximum conductance rather than a change in affinity for the malate substrate. The dependence of the magnitude of the GmALMT1-mediated steady-state inward currents on increasing $\{mal^{2-}\}_i$ shown in Figure 8, A to C, was also accompanied by a positive shift in the holding potential at which the current reverses sign (E_{rev}) of about −15 mV as $\{mal^{2-}\}_i$ was increased to 4.5 mM (data not shown). Comparison of the current-to-voltage relations generated by a voltage ramp protocol with GmALMT1-expressing cells confirmed that an increase in $\{mal^{2-}\}_i$ resulted in a significant shift in E_{rev} toward more positive potentials (Fig. 8D). In contrast, control cells showed no significant shift in the reversal potential upon increasing $\{mal^{2-}\}_i$. At low pH values, the transport activity of GmALMT1 was independent of the presence or absence of Al^{3+} (100 μM $AlCl_3$) in the bath medium (data not shown). Overall, the increase in inward current upon increasing $\{mal^{2-}\}_i$ and the concomitant positive shift in E_{rev} are consistent with GmALMT1-mediated inward currents being the product of anion efflux, ultimately indicating that at physiologically relevant membrane potentials, GmALMT1 functions as a transporter capable of mediating malate efflux from the cell. Furthermore, the pH dependence of the transporter (i.e. lower transport rates at lower pH) suggests that, in addition to changes in gene expression, the pH dependence of the whole-root malate exudation described above (Fig. 3A) is quite likely also the product of the functional characteristics of the GmALMT1 transporter mediating this process in planta in response to lowering the pH of the solution bathing the root.

Overexpression of *GmALMT1* in Transgenic Arabidopsis Plants Confers Al Tolerance

The function of GmALMT1 was further investigated in two Arabidopsis transgenic lines (OX1 and OX2) overexpressing *GmALMT1*. Quantification of *GmALMT1* transcript abundance in the two transgenic lines by qRT-PCR indicated that *GmALMT1* was highly expressed in these transgenic lines but not in control lines (Fig. 9A). These two overexpression lines showed significantly larger root malate exudation rates and superior Al tolerance (as determined by relative root growth) compared with the control (Fig. 9, B–D). These results clearly demonstrate that overexpression of *GmALMT1* in Arabidopsis promotes root malate release, thereby conferring a significant increase in Al tolerance.

GmALMT1 Mediates Malate Exudation and Determines Al Tolerance in Soybean Transgenic Hairy Roots

The role of GmALMT1 as a malate efflux transporter was further verified in transgenic soybean hairy roots

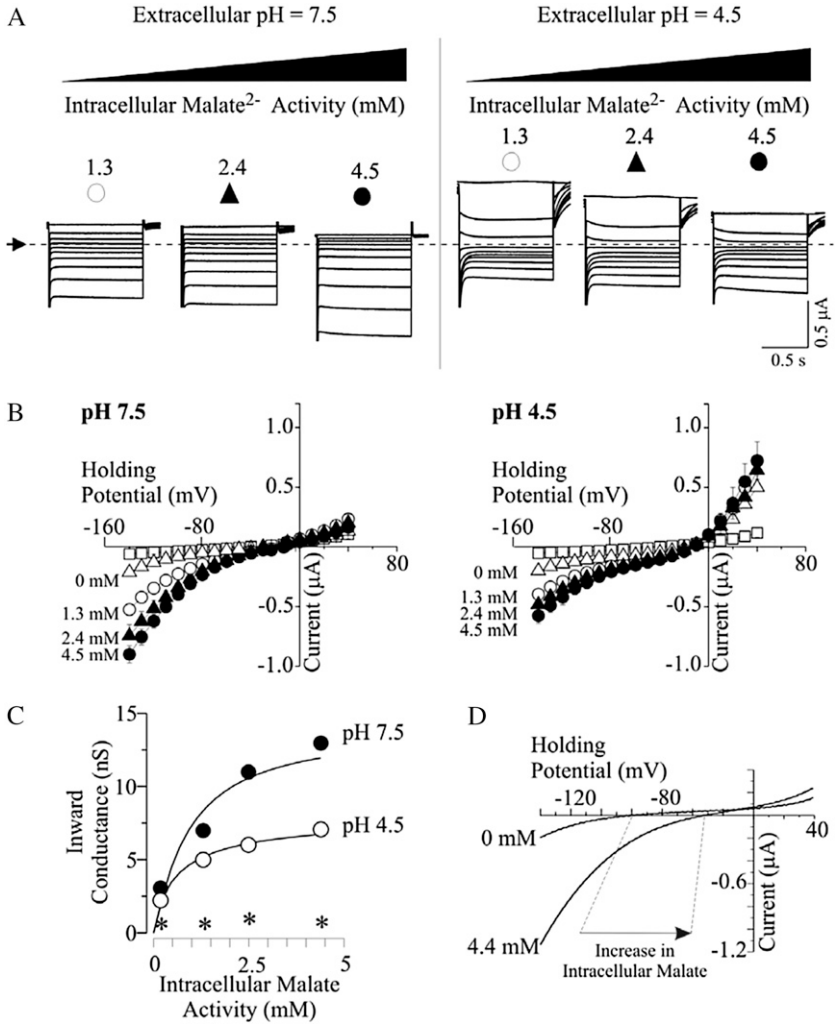

Figure 8. Effects of intracellular malate activities and extracellular pH on GmALMT1-mediated currents expressed in *X. laevis* oocytes. Two to 3 h prior to the electrophysiological measurements, cells were preloaded with 50 nL of sodium-malate solution (pH 7.2), resulting in internal malate free activities ranging from 0 to 4.5 mM. A, Example of GmALMT1-mediated currents elicited in response to the voltage protocol described in Figure 7B, as extracellular pH (7.5, left panel; 4.5, right panel) and $\{mal^{2-}\}_i$ (denoted on the top of each set of traces) were varied. The dotted line and arrow on the left margin indicates the zero-current level. B, Mean current-voltage curves constructed from the steady-state current recordings such as those shown in A for GmALMT1-expressing cells at various $\{mal^{2-}\}_i$ in standard bath solutions at pH 7.5 (left panel) and 4.5 (right panel). The symbols correspond to those depicted above the example traces in A. Values for control cells (white squares) and GmALMT1 cells not preloaded with malate (white triangles) correspond to those shown in Figure 7. C, Analysis of GmALMT1-mediated inward conductances in response to changes in extracellular pH and increasing $\{mal^{2-}\}_i$. The inward conductances were estimated by the linear regression of the current at the four most negative potentials. The curves were drawn according to the Hill equation: $G = G_{max} \times [(mal_i)^n/[(mal_i)^n] + K^n]$, where (mal_i) stands for the internal malate activity, G_{max} is the maximum conductance, and K is the internal malate activity where the conductance reaches one-half of its maximum value. Best fit resulted in K = 0.9 ± 0.2 mM, G_{max} = 14 ± 1 nS, and n = 1.1 ± 0.32 (r^2 = 0.934) at pH 7.5 and K = 0.6 ± 0.1 mM, G_{max} = 8 ± 1 nS, and n = 0.87 ± 0.11 (r^2 = 0.988) at pH 4.5. The inward slope conductance for control cells at pH 4.5 is indicated by the asterisks. D, The increase in the magnitude of the GmALMT1-mediated inward current upon increasing intracellular malate is concurrent with a positive shift in the reversal potential (E_{rev}; noted by the dashed lines). Whole-cell currents were elicited by a voltage ramp protocol from −140 to + 40 mV (0.9-s duration), from a holding potential of +40 mV, in standard bath solution (pH 7.5). The currents shown are representative of those obtained in ramp trials of cells (n = 5) not loaded (0 mM) or preloaded (n = 6) with malate ($\{mal^{2-}\}_i$ = 4.5 mM), as indicated next to each ramp.

overexpressing *GmALMT1* (GmALMT1-OX) and with reduced *GmALMT1* expression via RNA interference (GmALMT1-KD). The *GmALMT1* transcript abundance for these transgenic lines was confirmed via qRT-PCR (Fig. 10A). *GmALMT1* transcript abundance was 1.4 times higher in the GmALMT1-OX lines compared with the control line, while the transcript levels in the GmALMT1-KD lines were 50% lower than those in the control. As shown in Figure 10B, the malate exudation rates from the hairy roots of these lines

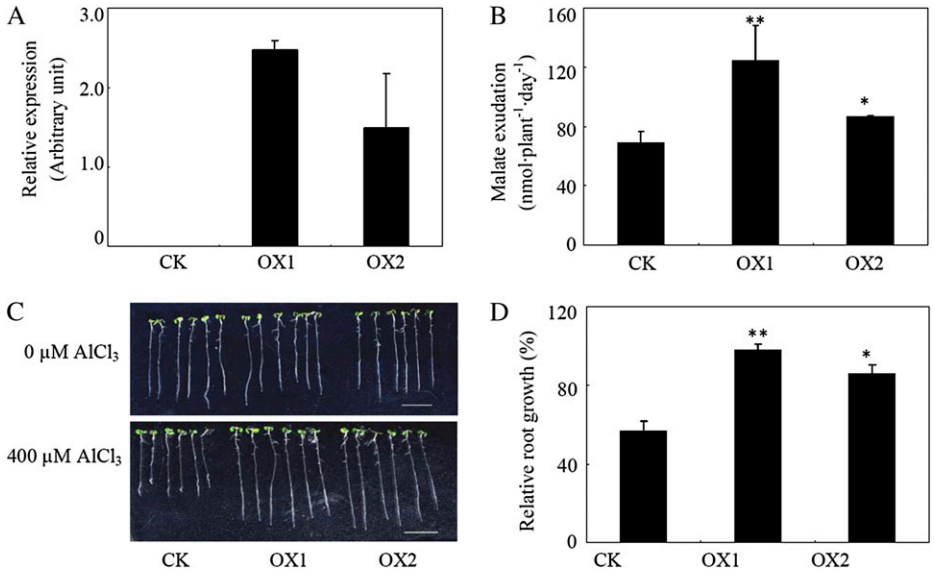

Figure 9. Al tolerance is enhanced by heterologous expression of *GmALMT* in transgenic Arabidopsis plants. A, *GmALMT1* expression in the two transgenic lines (OX1 and OX2) and a control line (CK). B, Malate exudation of transgenic Arabidopsis and control plants under low-pH conditions. C, Root growth performance. D, Relative root growth of the plants subjected to 400 μM Al for 2 d. All the data represent means of four replicates ± SE. Asterisks indicate significant differences from the control: $*P < 0.05$, $**0.001 < P < 0.01$.

were closely correlated with the level of *GmALMT1* expression, being 58% lower in the GmALMT1-KD lines and 87% greater in the GmALMT1-OX lines, relative to those measured in the control. The function of GmALMT1 related to Al tolerance was also quantified in soybean transgenic hairy roots. As this hairy root system is not amenable to relative root growth measurements, root Al exclusion measured with the Al stain hematoxylin was used as a physiological measure of Al tolerance. After 3 h of exposure to 50 μM Al, the hairy roots of the GmALMT1-OX lines accumulated less Al in the root tips than control roots, as indicated by the degree of hematoxylin staining on the surface of the root tips (Fig. 10C). Overall, these results strongly suggest that GmALMT1 does function as a malate efflux transporter in soybean roots, chelating free Al at the root surface and excluding it from entering the root system, thereby providing Al tolerance.

DISCUSSION

Highly acidic soil pH, high Al, and low P availability are the three major limiting factors in acid soils, which constitute up to 40% of world arable land and severely inhibit world crop production (Kochian et al., 2004). Although it has been reported that crops such as rice, maize, and common bean (*Phaseolus vulgaris*) have great genetic potentials for adaptation to acid soils, most of the phenotypic screening in these types of studies have been conducted either in the field or performed in the laboratory and have focused primarily on Al tolerance or occasionally on P efficiency (Cranados et al., 1992; Rao et al., 1993; Yan et al., 1995). Very few studies have simultaneously considered P availability and Al toxicity together (Zheng et al., 2005; Liao et al., 2006). Since soil pH, levels of rhizotoxic Al species, and P availability are not homogeneously distributed in acid soils, it is clear that plant roots have to deal with different levels of low pH, Al toxicity, and P availability during their growth through acidic soil horizons (Supplemental Table S1; Liao et al., 2006). Therefore, this study represents, to our knowledge, the first multidisciplinary study to focus on the combined effects of these three major limiting factors in acid soils to plant growth, implementing field evaluations and physiological, molecular, and biophysical analyses in the laboratory to elucidate the underlying mechanisms of crop adaptation to acid soils.

For crops to maintain growth on acid soils, they need to be adaptive to low pH (toxic levels of H^+), Al toxicity, and/or P deficiency (Kochian et al., 2004). Our field trials indicated that the P-efficient soybean genotype adapted better to acid soil conditions than the P-inefficient genotype, showing significantly greater biomass and longer total root length, especially under conditions of P supply (Fig. 1). Further studies in hydroponics also showed that the P-efficient soybean genotype exhibited greater tolerance to Al when P was supplied (Fig. 2), consistent with our previous report indicating that P-efficient soybean genotypes are more Al tolerant under P application (Liao et al., 2006). It should be noted here that the effect of P supply on enhancing Al tolerance was not simply due to the added Pi chelating Al^{3+} in the nutrient solution. Careful design of the hydroponic nutrient solutions using the ion speciation program GEOCHEM-EZ (Shaff et al., 2010) guaranteed that there were identical levels of free Al^{3+} activity in both +P and –P nutrient solutions. Our findings lead us to suggest that greater adaptation to acid soils may in part be the result of greater P efficiency as well as greater tolerance to Al toxicity and low pH. The underlying mechanisms associated with the P-efficient genotype only exhibiting better Al tolerance under conditions of sufficient P supply will be discussed later in this section.

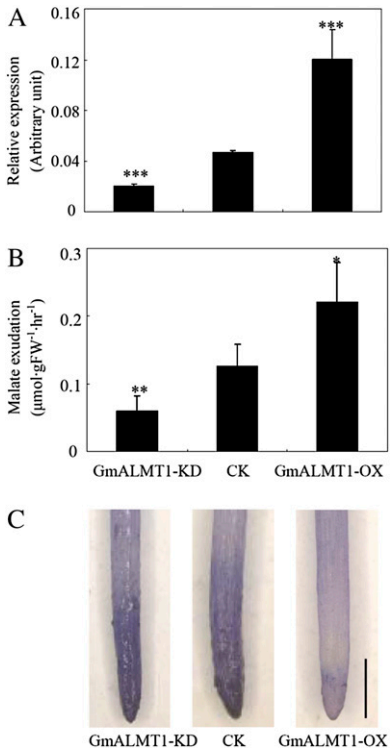

Figure 10. *GmALMT1* expression (A), malate exudation (B), and Al tolerance (C) of the composite soybean transgenic hairy roots under low-pH (pH 4.3) conditions. Root malate exudation was measured after the roots were exposed to 4.3 mM $CaCl_2$ (pH 4.3) for 6 h. Root tips stained with the Al stain, hematoxylin, was used as an indicator of Al tolerance. GmALMT1-KD and GmALMT1-OX represent *GmALMT1* RNA interference and overexpression lines, respectively. The lines transformed with empty vector were used as controls (CK). FW, Fresh weight. All the data are means of four biological replicates ± SE. Asterisks indicate significant differences: $*P < 0.05$, $**0.001 < P < 0.01$, $***P < 0.001$. Bar = 1 mm.

Previously, we found that malate exudation from the tips of the more deeply growing tap root of the P-efficient soybean genotype was specifically enhanced when the upper, more shallowly placed lateral roots were supplied with P while the tap root tip was challenged by Al, suggesting that P efficiency resulting in improved P nutrition plays a role in the malate exudation critical for Al tolerance (Liao et al., 2006). This hypothesis is also supported by the results from studies in rape, where it was shown that root malate exudation was up-regulated by the interactions of P and Al (Ligaba et al., 2004). Furthermore, several studies have also suggested that malate exudation and internal malate homeostasis could play vital roles in plant adaptation to low-pH stress, Al toxicity, or P deficiency (Hoffland et al., 1992; Martínez-Camacho et al., 2004; Sasaki et al., 2004). In this study, we used a hydroponic system to analyze the relationships between malate exudation and internal malate homeostasis in response to changes in solution pH as well as Al and P levels in the growth solution. Our results indicate that in control solution (pH 5.8, +P, −Al), root malate exudation was much higher than in the same solution adjusted to pH 4.3 (Fig. 3A). Similar responses have also been observed in other plant species (Bertin et al., 2003). High root malate release has been speculated to be involved in other plant responses to the environment, such as in interactions between plants and soil microorganisms (Walker et al., 2003; Rudrappa et al., 2008). This speculation has been supported by the fact that the roots of a sorghum cultivar with more efficient colonization of nitrogen-fixing free-living bacteria exude more malate (Krotzky et al., 1986, 1988). Hence, greater secretion of malate from soybean roots at less acidic pH might provide more carbon for beneficial microorganisms, such as rhizobia and mycorrhizal fungi. We also found that low pH significantly reduced both malate exudation and malate content in soybean root tips (Fig. 3). Reduction of malate content as a result of low-pH stress has also been reported in the roots of maize and broad bean (*Vicia faba*; Yan et al., 1992). It has been suggested that the reduction of malate content in plant roots might be caused by the decarboxylation of malate for stabilizing cytoplasmic pH when cytoplasmic acidification occurs due to roots growing in an acidic environment (Davies, 1973). Thus, the decreasing malate content of roots may constitute an adaptive change to low-pH stress. Moreover, the P-efficient genotype HN89 always maintained higher root malate content at low pH regardless of the P and Al levels in the solution (Fig. 3B), suggesting that it has a greater potential to adapt to acidic soil conditions.

The malate exudation in response to Pi starvation has been suggested as a mechanism for P mobilization in the soil in several plant species grown on acid soils (Hoffland et al., 1989; Hinsinger, 2001; Sas et al., 2001). Although we also observed that low-P-grown plants had a higher root malate exudation at low pH than did plants supplied with P, these differences were not as large as those described earlier (Fig. 3A). Increased malate exudation under low-P conditions can help to solubilize P that is fixed by iron and Al oxides in acid soils, thereby enhancing the plant's adaptation to P deficiency (Hoffland et al., 1992; Sas et al., 2001; Lü et al., 2012). More interestingly, under the combined conditions of low pH, Al toxicity, and high P availability in hydroponics, which mimics the conditions of acid soils fertilized at the soil surface with P, the decrease in malate exudation in soybean roots under low-pH conditions was alleviated by Al supply, particularly in the P-efficient genotype HN89 (Fig. 3A). These results strongly suggest that root malate exudation might be the critical mechanism for soybean adaptation to acid soils and that control of the expression of the gene encoding the malate transporter underlying these responses, as well as the activity of the transport protein, might be regulated both by Al exposure and plant P status as well as low external pH.

We cloned a malate transporter (designated *GmALMT1*) from soybean roots treated with Al using degenerate

primers derived from the conserved domain of previously cloned malate transporter proteins from wheat, Arabidopsis, and rape. The expression of *GmALMT1* was found to be regulated by low pH, Al toxicity, and P availability. *GmALMT1* expression was Al concentration dependent, and its expression was only upregulated by Al in soybean root tips and not in the mature root regions (Fig. 4, A and B). Since root tips are the primary site of Al toxicity where any primary Al tolerance mechanism must reside (Ryan et al., 1992; Delhaize et al., 1993a), this root tip-specific and Al concentration-dependent expression pattern is consistent with the role of GmALMT1 in the efficient detoxification of Al toxicity. The localization to the root tip will greatly reduce the carbon cost to the plant for this tolerance mechanism. Similar Al-activated expression patterns were also observed for *AtALMT1* and *BnALMT1* in Arabidopsis and rape, respectively (Hoekenga et al., 2006; Ligaba et al., 2006). Subcellular localization of GmALMT1 indicated that the protein is localized to the plasma membrane (Fig. 6). Functional analysis of GmALMT1 in *X. laevis* oocytes also demonstrated that GmALMT1 functions as a plasma membrane transporter capable of mediating malate efflux (Figs. 7 and 8). Although many ALMTs have been characterized, not all of them are involved in plant Al tolerance. The function of GmALMT1 as a malate transporter that mediates root malate exudation is analogous to the same proposed function for related ALMT1 proteins from barley, wheat, Arabidopsis, and rape (Sasaki et al., 2004; Hoekenga et al., 2006; Ligaba et al., 2006) but different from ZmALMT1 and ZmALMT2, which function as mineral anion transporters in maize (Piñeros et al., 2008b; Ligaba et al., 2012). GmALMT1 is also distinctly different from some other ALMT members, such as AtALMT12 and HvALMT1, which encode guard cell anion channels that facilitate organic anion transport involved in the opening and closing of stomatal complexes in leaves (Gruber et al., 2010; Meyer et al., 2010), or AtALMT9, which is localized to the vacuole, playing a role in the regulation of cytosolic malate homeostasis (Kovermann et al., 2007). In this study, we have also revealed that GmALMT1 activity is Al independent and its transport activity is highly dependent on extracellular pH (Fig. 8), a unique regulatory mechanism not yet described for other ALMT-type transporters. Interestingly, not only was GmALMT1 transport activity (Fig. 7) regulated by external pH, but also its expression in planta was downregulated by low pH (Figs. 4C and 5), which closely correlates with the reduction in root malate exudation when the roots are transferred from pH 5.8 to 4.3 (Fig. 3A). The response of *GmALMT1* to low pH makes *GmALMT1* quite distinctive from the other known *ALMT* genes involved in Al tolerance. In these other *ALMTs*, including *AtALMT1* and *TaALMT1*, their expression is not influenced by or is slightly increased in response to low-pH conditions (Sasaki et al., 2004; Kobayashi et al., 2007; Liu et al., 2009). When subjected to the conditions that mimic the acid soil syndrome of low pH, high Al, and variable P supply, the expression of *GmALMT1* was suppressed by low pH but increased by Al and P addition, especially for the P-efficient genotype HN89 (Fig. 5).

The functionality of *GmALMT1* was also investigated by overexpression in Arabidopsis as well as altering its expression in soybean using the soybean transgenic hairy root system. Overexpression of *GmALMT1* in both soybean hairy roots and Arabidopsis led to greater malate exudation (Figs. 9B and 10B), while knocking down the expression of *GmALMT1* in soybean hairy roots by RNA interference led to decreased malate exudation from hairy roots (Fig. 10B). Furthermore, in both Arabidopsis and soybean hairy roots, these genetically induced changes in *GmALMT1* expression, which led to the expected changes in malate exudation, correlated well with changes in Al tolerance. The strong correlation between the different experimental approaches provides solid evidence that GmALMT1 is a plasma membrane root malate efflux transporter that plays a critical role in soybean Al tolerance.

Based on field evaluations as well as physiological and molecular analyses in the laboratory, we conclude that root malate exudation in soybean is coordinately regulated by low pH, Al, and P through *GmALMT1*, which might be the critical mechanism for soybean adaptation to acid soils. Therefore, *GmALMT1* could be considered as a potential candidate gene for crop improvement in acid soils through biotechnological approaches.

MATERIALS AND METHODS

Plant Materials and Growth Conditions

Two soybean (*Glycine max*) genotypes, HN89 and HN112, contrasting in P efficiency were used in this study. A previous study from our laboratory established that HN89 is a P-efficient genotype while HN112 is a P-inefficient genotype (Zhao et al., 2004).

In the field trial, soybean plants were grown on acidic red soils at the Boluo (E114.28°, N23.18°) field site in Guangdong Province, China. Basic soil chemical characteristics of the top 20-cm layer were as follows: pH, 5.71; organic matter, 1.76 mg kg^{-1}; available P (Bray I method), 12.31 mg kg^{-1}; available nitrogen, 86.64 mg kg^{-1}; available potassium, 75.28 mg kg^{-1}. There were two P treatments: low P (no P added) and high P (80 kg P_2O_5 ha^{-1} added as triple superphosphate to the top 10 cm of soil by band application). Concentrations of 80 kg nitrogen ha^{-1} as urea and 80 kg potassium kg^{-1} as KCl were used to supply nitrogen and potassium for all plants. The soil samples were separately taken from three layers (0–20, 20–40, and 40–60 cm) along the soil profile before planting, and their pH values, exchangeable acidity, and exchangeable P and Al^{3+} content were measured. The trial was conducted using a randomized block design with six replicates for each treatment. Sixty days after sowing, soybean plants were harvested and total root length and dry weight were determined (Zhao et al., 2004). After being carefully washed, roots were scanned and the total root length was quantified with computer image-analysis software (WinRhizo Pro; Régent Instruments).

For the hydroponics studies, soybean seeds were sterilized with 10% (v/v) bleach for 1 min and germinated in paper rolls in a beaker at 25°C. To maintain the moisture of the germination paper rolls, 1 to 2 cm of one-fourth-strength modified Hoagland nutrient solution (pH 5.8) was added into the beaker (Liao et al., 2006). At 3 d after germination, the seedlings were transferred to 0.5 mM $CaCl_2$ with corresponding Al concentration to study the *GmALMT1* expression pattern as related to Al and pH value. To test the spatial expression patterns of *GmALMT1* in roots, root regions of 0 to 2, 2 to 4, and more than 4 cm from the

root tips were separately harvested for qRT-PCR analysis after 6 h of Al exposure. For analyzing dose effects of Al toxicity on *GmALMT1* expression, roots of HN89 were exposed to 0, 50, and 100 μM $AlCl_3$ for 6 h. The first 2-cm root segments from root tips were harvested for qRT-PCR analysis. For assaying temporal expression patterns of *GmALMT1* as related to low pH and Al toxicity, seedlings of HN89 were treated with low pH (4.3) for 12 h. For the non-Al-treated samples, the first 2-cm root segments from the root tips were harvested at 0, 6, and 12 h. For the Al treatment samples, after 12 h of low-pH acclimation, the seedlings were transferred to 50 μM $AlCl_3$. Root tips were harvested at 2, 4, 6, 8, 10, 12, and 24 h of Al treatment.

To investigate the effects of Al, P, and low pH on the expression of *GmALMT1*, root growth, malate exudation, and root tip malate content, soybean seeds were germinated separately in P-sufficient (250 μM KH_2PO_4) and P-deficient (5 μM KH_2PO_4) modified Hoagland nutrient solution (pH 5.8) for 3 d. After germination, seedlings were subjected to fresh nutrient solution with specific pH, Al, and P treatments, which partially mimic the real nutrient situation in acid soils. The two pH treatments were pH 4.3 and 5.8. The two P treatments were application of 320 μM (+P) or 0 μM (−P) KH_2PO_4. For Al treatments, seedlings were treated with (+Al) or without (−Al) 38 μM Al^{3+} activity as calculated by the GEOCHEM-EZ speciation software (Shaff et al., 2010). The combinations of the treatments were +Al/+P/pH 4.3, +Al/−P/pH 4.3, −Al/+P/pH 4.3, −Al/+P/pH 5.8, −Al/−P/pH 5.8 and −Al/−P/pH 5.8. After 6 h of treatment, the first 2-cm tap root tips were harvested for quantifying *GmALMT1* expression. Relative root length was measured using rulers and determined by the percentage of relative net root growth as described before, using tap root growth under the treatments including −Al/+P/pH 5.8 and −Al/−P/pH 5.8 as controls (Liu et al., 2009). In order to minimize the interference of other nutrient elements in the capillary electrophoresis determinations of malate as well as to reduce the stress of low ion strength, measurements of malate exudation and accumulation were performed in 4.3 mM $CaCl_2$ solution. Soybean seedlings were directly transferred to 4.3 mM $CaCl_2$ solution including the two P levels (0 and 320 μM KH_2PO_4), two pH levels (4.3 and 5.8), and two Al levels (0 and 38 μM Al^{3+} activity), as mentioned above. All the hydroponic experiments were aerated according to Liao et al. (2006). All the treatments had four replicates.

Determination of Malate Exudation and Accumulation

To quantify malate exudation from soybean roots, seedlings of both soybean genotypes were subjected to the specific treatments. For all the treatments of Al toxicity, the pH value of the solution was adjusted to 4.3. After 6 h of treatment, root exudates were collected and frozen at −20°C for further analysis. The first 2 cm from the tips of the tap roots was then harvested for root malate content determinations. Each treatment for different genotypes included four replicates, with each replicate containing four plants.

Secreted malate was processed and measured as described before (Liao et al., 2006). Briefly, the root exudates were passed through a silver cartridge (OnGuardII Ag; Dionex) to remove excess Cl^-. The pass-through products were then mixed with cation-exchange resin (100:1, v/w) for 10 min to remove cations and make the organic acids fully quantifiable. Following centrifugation, the supernatants were used for malate determination. In order to determine malate content in root tips, root tips were extracted using 18-Ω water. After centrifuging at 12,000 rpm for 10 min at 4°C, the supernatants were collected and used for malate content measurement. Malate determinations were conducted on a Beckman-Coulter MDQ capillary electrophoresis system using methods more fully described by Maron et al. (2010).

Isolation and Characterization of *GmALMT1*

Total RNA was extracted from the root tips of the P-efficient soybean genotype HN89 subjected to Al toxicity. The degenerate primers (5′-TGGGCIRTIHTIACIGTIGT-3′ and 5′-CCIGCCCAIAYIGGRMA-3′) were designed according to the conserved motifs of ALMTs from Arabidopsis (*Arabidopsis thaliana*), rape (*Brassica napus*), and wheat (*Triticum aestivum*). A fragment of 405 bp was PCR amplified using the degenerate primers from the cDNA. Subsequently, 5′ and 3′ ends of *GmALMT1* were separately amplified using RACE following the Advantage 2 PCR Kit manual (Clontech) using the following primers (5′-GCCTCTTTATGATGGCTTCGGAGTTG-3′, 5′-AATGTGGGCTGTTCTGACAGTGGTG-3′, 5′-CAAGTACTGCTCCCAAGGATGGCGA-3′, and 5′-GACGGGACAAATGAAAGTGGAGATGACC-3′). All the PCR fragments were cloned into a pGEM-T Easy vector (Promega) for sequence confirmation. These fragments were analyzed and combined to generate a full-length cDNA through the MEGA 4.1 program. Phylogenetic tree analysis was performed with MEGA4.1.

Characterization of *GmALMT1* Expression

The expression of *GmALMT1* was determined by qRT-PCR. Briefly, total RNA was extracted using Trizol reagent according to the manual (Invitrogen) and treated with DNase I (Invitrogen). Two micrograms of total RNA from each sample was used for the first-strand cDNA synthesis in a 20-μL reverse transcription reaction. Reverse transcription was performed according to the manufacturer's protocol (Invitrogen). The first-strand cDNA was used for SYBR Green-monitored qRT-PCR (ABI). The qRT-PCR analysis was performed using the Applied Biosystems 7500 Real-Time PCR System (ABI). The primer pairs used for qRT-PCR analysis for *GmALMT1* were 5′-GAGCACTTACTCGGGAATGTG-3′ and 5′-GGACTTTGGCAGTTG ATGGG-3′, and those for the housekeeping gene *EF-1α* were 5′-TGCAAAGGAGGCTGCTAACT-3′ and 5′-CAGCATCACCGTTCTTCAAA-3′. The expression of *GmALMT1* was calculated from the relative expression levels of *GmALMT1* and the expression levels of the reference gene *EF-1* using arbitrary units.

Subcellular Localization of the GmALMT1-YFP Fusion Protein

Subcellular localization was determined via the transient expression of translational fusions with YFP in Arabidopsis leaf protoplasts. The coding regions (cDNA) of *GmALMT1* were subcloned into the expression vector pSAT6-eYFP-C1 (Tzfira et al., 2005). Transient expression of the YFP::GmALMT1 translational fusion was carried out as described (Yoo et al., 2007). Protoplasts were transformed with 20 μg of plasmid DNA via polyethylene glycol transformation and incubated in the dark at room temperature overnight. Plasma membrane staining was achieved by incubation of protoplasts with CellMask Orange (Invitrogen; www.invitrogen.com) at a concentration of 2.5 μg mL^{-1} for 15 min at 30°C. Imaging was conducted with a Leica TCS SP5 laser scanning confocal microscope (www.leica-microsystems.com). The excitation/emission filter wavelengths for each channel were as follows: GFP, 488/500 to 525 nm; CellMask plasma membrane dye, 561/570 to 586 nm; chloroplast autofluorescence, 561/669 to 694 nm.

Functional Characterization of GmALMT1 in *Xenopus laevis* Oocytes

The coding region of *GmALMT1* was cloned between the *Bgl*II and *Spe*I unique site of the T7TS plasmid. The coding region contained a kosak consensus sequence (GCCGCCACC) immediately upstream of the initiation codon and was flanked by the 3′ and 5′ untranslated regions of an *X. laevis* β-globin gene. The construct was fully sequenced and checked for sequence accuracy. cRNA was synthesized from 1 μg of *Sma*I-linearized plasmid DNA template using the mMessage in vitro transcription kit (Ambion; http://www.ambion.com/) according to the manufacturer's recommended procedures and purified with the MegaClear kit (Ambion), eluted in RNase-free water, and stored at −80°C. Harvested and defolliculated stage V and VI *X. laevis* oocytes were maintained as described previously (Piñeros et al., 2008a). Oocytes were injected with 50 nL of water or 50 nL of water containing 30 ng of GmALMT1 cRNA and incubated in ND96 (Piñeros et al., 2008a) at 18°C for 2 to 3 d prior to electrophysiological measurements.

Whole-cell currents were recorded under constant perfusion with both GeneClamp 500 and Axoclamp900A amplifiers (Axon Instruments; http//www.moleculardevices.com/homr.html) using the two-electrode voltage clamp technique. The recording electrodes were filled with 0.5 M K_2SO_4 and 30 mM KCl and had resistances between 0.5 and 1.5 MΩ. The standard bath recording solution contained (in mM) 96 NaCl, 1 KCl, 1.8 $CaCl_2$, and 0.1 $LaCl_3$ with the pH adjusted to 7.5 or 4.5. $LaCl_3$ was included in the bath solution as it effectively attenuates potential voltage-dependent, hyperpolarization-induced, and volume-sensitive endogenous oocyte chloride currents (Ackerman et al., 1994; Tokimasa and North, 1996). The latter approach has been successful for the characterization of inward currents mediated by several members of the ALMT family of transporters (Hoekenga et al., 2006; Piñeros et al., 2008a; Ligaba et al., 2012). It is worth noting that acidification of the bath medium can result in highly variable increases in the endogenous outward currents at holding potentials more positive than +60 mV. Thus, currents under voltage

clamp conditions were elicited by 1-s voltage pulses in 10-mV step increments between +40 and −140 mV, with a 10-s rest at +40 mV between voltage pulses. The output signal was digitized and analyzed using Digidatas1320A and 1440APClamp 10 data-acquisition systems (Axon Instruments). The steady-state current-voltage relationships were constructed by measuring the current amplitude at the end of the test pulse. All data points represent means ± SE of at least eight different cells from two to three donor frogs. Error bars denote SE and are not shown when they are smaller than the symbol. Intracellular malate concentrations were modified by injecting 50 nL of varying concentrations (0–100 mM) of sodium malate, resulting in expected free $\{mal^{2-}\}_i$ values of 1.3, 2.4, and 4.5 as described previously (Piñeros et al., 2008a; Ligaba et al., 2012). Slope conductances of the inward currents were estimated by the linear regression of current values between −140 and –100 mV.

Heterologous Expression of *GmALMT1* in Arabidopsis

A binary plasmid vector was constructed for stable plant transformation with the *GmALMT1* gene under the control of the cauliflower mosaic virus 35S. The coding region of *GmALMT1* was amplified with primers (5′-GGAAGATCTCATGGATATAGAGTCAACAACCCAAGC-3′ and 5′-CAGCACGCGTCTATTTACAAATTGAATGTTCCGAGGG-3′) and subcloned into the *Bgl*II/*Mlu*I site of the pYLRNAi vector (Liang et al., 2010). The construct was then transformed into the *Agrobacterium tumefaciens* strain GV3101 by electroporation, which was then used for Arabidopsis transformation. The expression of *GmALMT1* in the transgenic plants was qualified by qRT-PCR. The Arabidopsis tubulin gene was used as the internal control using the following two primers (5′-TGTCGTCCAACCTTACAACTCACT-3′ and 5′-TCTCCAGGGTCCTCCATTCC-3′).

Two representative transgenic homozygous T3 lines were used for determining malate exudation and Al tolerance. In the transgenic Arabidopsis plants, Al tolerance was determined by measuring relative root growth. For malate exudation assays, Arabidopsis seeds were surface sterilized and germinated on solid Murashige and Skoog medium for 1 week. Uniform seedlings were then transferred to hydroponic Murashige and Skoog medium and grown with shaking at 180 rpm. After 10 d of incubation, seedlings were washed several times with sterilized water and the growth medium was replaced by a solution consisting of 0.5 mM $CaCl_2$ (pH 4.3) and no Al, in order to minimize interference from the endogenous AtALMT1 Al-dependent malate exudation present in Arabidopsis. After 24 h of incubation, the collection solution was sampled for malate assay. To quantify root growth and the effect of Al toxicity, seeds of wild-type Arabidopsis and two transgenic lines were surface sterilized and germinated for 4 d on solid Murashige and Skoog medium. After germination, uniform seedlings were transferred to 0.5 mM $CaCl_2$-agar plates containing 0 or 400 μM $AlCl_3$. After 2 d of treatments, plant roots were scanned, and primary root length was measured using the ImageJ program. The relative root growth was calculated as described (Liu et al., 2009). Each treatment for different lines had four replicates, each of which contained four plants.

Overexpression and Knockdown via RNA Interference of *GmALMT1* in Soybean Hairy Roots

The *GmALMT1* transformation vector described above was also used for *GmALMT1* expression in soybean hairy roots. The RNA interference construct was made by amplifying the coding region of *GmALMT1* with primers (GmMT1RiB, 5′-GGATCCTGGTCGCTGTCTCG-3′; GmMT1RiH, 5′-AAGCTTACATTCCCGAGTAAGTGCT-3′; GmMT1RiP, 5′-CTGCAGACATTCCCGAGTAAGTGCT-3′; and GmMT1RiM, 5′-ACGCGTTGGTCGCTGTCTCG-3′) and subcloned into the pYLRNAi vector (Liang et al., 2010). The constructs were then transformed into the *Agrobacterium rhizogenes* strain K599, which was used for soybean hairy root transformation.

The transgenic soybean composite plants with wild-type shoots and transgenic roots were developed according to Kereszt et al. (2007). Soybean hairy roots transformed with empty vectors were used as controls. The hairy roots from 3 weeks after transformation were used for further analysis. RNA was extracted from hairy roots, and qRT-PCR was used to quantify the *GmALMT1* expression in both transgenic lines and the control lines. Four independent lines of each construct were used for the determination of malate exudation. Composite plants were exposed to 4.3 mM $CaCl_2$ (pH 4.3) for 6 h, and root exudates were collected and processed for the malate measurement. To detect the function of GmALMT1 as related to Al detoxification, soybean hairy roots were subjected to 0.5 mM $CaCl_2$ (pH 4.3) containing 50 μM Al. After 3 h of incubation, the hairy roots were then stained with hematoxylin as described by Delhaize et al. (1993a). Briefly, the hairy root tips were first washed for 30 min with distilled water and then stained with hematoxylin for 30 min. After staining, the root tips were washed for a further 30 min in distilled water and then photographed.

Statistical Analysis

All of the data were analyzed statistically using Microsoft Excel 2000 for calculating means and SE and using SAS (SAS Institute) for ANOVA and Pearson linear correlation analysis between malate exudation and *GmALMT1* expression.

Supplemental Data

The following materials are available in the online version of this article.

Supplemental Figure S1. Phylogenetic tree of soybean ALMTs along with other plant ALMTs.

Supplemental Table S1. Conditions of acidity, Al, and P in the acid soils at the Boluo (E114.28°, N23.18°) field site in Guangdong Province, China.

ACKNOWLEDGMENTS

We thank Dr. Huicong Wang for her advice on organic acid analysis and quantification and Mr. Zuotong He for help in field management.

Received October 11, 2012; accepted January 18, 2013; published January 22, 2013.

LITERATURE CITED

Ackerman MJ, Wickman KD, Clapham DE (1994) Hypotonicity activates a native chloride current in *Xenopus* oocytes. J Gen Physiol **103:** 153–179

Archambault DJ, Zhang GC, Taylor GJ (1997) Spatial variation in the kinetics of aluminium (Al) uptake in roots of wheat (*Triticum aestivum* L.) exhibiting differential resistance to Al: evidence for metabolism dependent exclusion of Al. J Plant Physiol **151:** 668–674

Basu U, Good AG, Aung T, Slaski J, Basu A, Briggs KG, Taylor GJ (1999) A 23-kDa root exudates polypeptide co-segregates with aluminum resistance in *Triticum aestivum*. Physiol Plant **106:** 53–61

Bertin C, Yang X, Weston L (2003) The role of root exudates and allelo chemicals in the rhizosphere. Plant Soil **256:** 67–83

Cranados G, Pandey S, Ceballos H (1992) Response to selection for tolerance to acid soils in a tropical maize population. Crop Sci **33:** 936–940

Davies DD (1973) Control of and by pH. Symp Soc Exp Biol **27:** 513–529

Degenhardt J, Larsen PB, Howell SH, Kochian LV (1998) Aluminum resistance in the Arabidopsis mutant *alr-104* is caused by an aluminum-induced increase in rhizosphere pH. Plant Physiol **117:** 19–27

Delhaize E, Craig S, Beaton CD, Bennet RJ, Jagadish VC, Randall PJ (1993a) Aluminum tolerance in wheat (*Triticum aestivum* L.). I. Uptake and distribution of aluminum in root apices. Plant Physiol **103:** 685–693

Delhaize E, Ryan PR, Randall PJ (1993b) Aluminium tolerance in wheat (*Triticum aestivum* L.). II. Aluminium-stimulated excretion of malic acid from root apices. Plant Physiol **103:** 695–702

Delhaize E, Taylor P, Hocking PJ, Simpson RJ, Ryan PR, Richardson AE (2009) Transgenic barley (Hordeum vulgare L.) expressing the wheat aluminium resistance gene (TaALMT1) shows enhanced phosphorus nutrition and grain production when grown on an acid soil. Plant Biotechnol J **7:** 391–400

Dong D, Peng X, Yan X (2004) Organic acid exudation induced by phosphorus deficiency and/or aluminium toxicity in two contrasting soybean genotypes. Physiol Plant **122:** 190–199

Elstner EF, Wagner GA, Schutz W (1988) Activated oxygen in green plants in relation to stress situations. Curr Top Plant Biochem Physiol **7:** 159–187

Fukuda T, Saito A, Wasaki J, Shinano T, Osaki M (2007) Metabolic alterations proposed by proteome in rice roots grown under low P and high Al concentration under low pH. Plant Sci **172:** 1157–1165

Gaume A, Machler F, Frossard E (2001) Aluminum resistance in two cultivars of *Zea mays* L: root exudation of organic acid and influence of phosphorus nutrition. Plant Soil **234:** 73–81

Gruber BD, Ryan PR, Richardson AE, Tyerman SD, Ramesh S, Hebb DM, Howitt SM, Delhaize E (2010) HvALMT1 from barley is involved in the transport of organic anions. J Exp Bot **61:** 1455–1467

Hinsinger P (2001) Bioavailability of soil inorganic P in the rhizosphere as affected by root-induced chemical changes: a review. Plant Soil **237:** 173–195

Hoekenga OA, Maron LG, Piñeros MA, Cançado GMA, Shaff J, Kobayashi Y, Ryan PR, Dong B, Delhaize E, Sasaki T, et al (2006) *AtALMT1*, which encodes a malate transporter, is identified as one of several genes critical for aluminum tolerance in *Arabidopsis*. Proc Natl Acad Sci USA **103:** 9738–9743

Hoffland E, Findenegg GR, Nelemans JA (1989) Utilization of rock phosphate by rape. Plant Soil **113:** 155–160

Hoffland E, Van den Boogard R, Nelemans J, Findenegg G (1992) Biosynthesis and root exudation of citric and malic acids in phosphate-starved rape plants. New Phytol **122:** 675–680

Horst WJ, Schmoh N, Kollmeier M, Balulška F, Sivaguru M (1999) Does aluminium affect root growth of maize through interaction with the cell wall-plasma membrane-cytoskeleton continuum? Plant Soil **215:** 163–174

Huang CF, Yamaji N, Ma JF (2010) Knockout of a bacterial-type ATP-binding cassette transporter gene, *AtSTAR1*, results in increased aluminum sensitivity in Arabidopsis. Plant Physiol **153:** 1669–1677

Huang CF, Yamaji N, Mitani N, Yano M, Nagamura Y, Ma JF (2009) A bacterial-type ABC transporter is involved in aluminum tolerance in rice. Plant Cell **21:** 655–667

Iuchi S, Koyama H, Iuchi A, Kobayashi Y, Kitabayashi S, Kobayashi Y, Ikka T, Hirayama T, Shinozaki K, Kobayashi M (2007) Zinc finger protein STOP1 is critical for proton tolerance in *Arabidopsis* and coregulates a key gene in aluminum tolerance. Proc Natl Acad Sci USA **104:** 9900–9905

Jemo M, Abaidoo RC, Nolte C, Horst WJ (2007) Aluminum resistance of cowpea as affected by phosphorus-deficiency stress. J Plant Physiol **164:** 442–451

Kereszt A, Li D, Indrasumunar A, Nguyen CD, Nontachaiyapoom S, Kinkema M, Gresshoff PM (2007) *Agrobacterium rhizogenes*-mediated transformation of soybean to study root biology. Nat Protoc **2:** 948–952

Kinraide TB (1998) Three mechanisms for the calcium alleviation of mineral toxicities. Plant Physiol **118:** 513–520

Kinraide TB (2003) Toxicity factors in acidic forest soils: attempts to evaluate separately the toxic effects of excessive Al^{3+} and H^+ and insufficient Ca^{2+} and Mg^{2+} upon root elongation. Eur J Soil Sci **54:** 323–333

Kobayashi Y, Hoekenga OA, Itoh H, Nakashima M, Saito S, Shaff JE, Maron LG, Piñeros MA, Kochian LV, Koyama H (2007) Characterization of *AtALMT1* expression in aluminum-inducible malate release and its role for rhizotoxic stress tolerance in Arabidopsis. Plant Physiol **145:** 843–852

Kochian LV, Hoekenga OA, Pińeros MA (2004) How do crop plants tolerate acid soils? Mechanisms of aluminum tolerance and phosphorous efficiency. Annu Rev Plant Biol **55:** 459–493

Kovermann P, Meyer S, Hörtensteiner S, Picco C, Scholz-Starke J, Ravera S, Lee Y, Martinoia E (2007) The *Arabidopsis* vacuolar malate channel is a member of the ALMT family. Plant J **52:** 1169–1180

Koyama H, Toda T, Hara T (2001) Brief exposure to low-pH stress causes irreversible damage to the growing root in Arabidopsis thaliana: pectin-Ca interaction may play an important role in proton rhizotoxicity. J Exp Bot **52:** 361–368

Krotzky A, Berggold R, Werner D (1986) Analysis of factors limiting associative N_2-fixation (C_2H_2 reduction) with two cultivars of *Sorghum* mutants. Soil Biol Biochem **18:** 201–207

Krotzky A, Berggold R, Werner D (1988) Plant characteristics limiting associative N_2-fixation (C_2H_2 reduction) with two cultivars of *Sorghum* mutants. Soil Biol Biochem **20:** 157–162

Larsen PB, Degenhardt J, Tai CY, Stenzler LM, Howell SH, Kochian LV (1998) Aluminum-resistant Arabidopsis mutants that exhibit altered patterns of aluminum accumulation and organic acid release from roots. Plant Physiol **117:** 9–18

Liang CY, Tian J, Lam HM, Lim BL, Yan XL, Liao H (2010) Biochemical and molecular characterization of PvPAP3, a novel purple acid phosphatase isolated from common bean enhancing extracellular ATP utilization. Plant Physiol **152:** 854–865

Liao H, Wan H, Shaff J, Wang X, Yan X, Kochian LV (2006) Phosphorus and aluminum interactions in soybean in relation to aluminum tolerance: exudation of specific organic acids from different regions of the intact root system. Plant Physiol **141:** 674–684

Ligaba A, Katsuhara M, Ryan PR, Shibasaka M, Matsumoto H (2006) The *BnALMT1* and *BnALMT2* genes from rape encode aluminum-activated malate transporters that enhance the aluminum resistance of plant cells. Plant Physiol **142:** 1294–1303

Ligaba A, Maron LG, Shaff J, Kochian LV, Piñeros MA (2012) Maize ZmALMT2 is a root anion transporter that mediates constitutive root malate efflux. Plant Cell Environ **35:** 1185–1200

Ligaba A, Shen H, Shibata K, Yamamoto Y, Tanakamaru S, Matsumoto H (2004) The role of phosphorus in aluminium-induced citrate and malate exudation from rape (Brassica napus). Physiol Plant **120:** 575–584

Lipton DS, Blanchar RW, Blevins DG (1987) Citrate, malate, and succinate concentration in exudates from P-sufficient and P-stressed *Medicago sativa* L. seedlings. Plant Physiol **85:** 315–317

Liu J, Magalhaes JV, Shaff J, Kochian LV (2009) Aluminum-activated citrate and malate transporters from the MATE and ALMT families function independently to confer *Arabidopsis* aluminum tolerance. Plant J **57:** 389–399

Lü J, Gao X, Dong Z, Yi J, An L (2012) Improved phosphorus acquisition by tobacco through transgenic expression of mitochondrial malate dehydrogenase from *Penicillium oxalicum*. Plant Cell Rep **31:** 49–56

Ma JF (2000) Role of organic acids in detoxification of aluminum in higher plants. Plant Cell Physiol **41:** 383–390

Ma JF, Taketa S, Yang ZM (2000) Aluminum tolerance genes on the short arm of chromosome 3R are linked to organic acid release in *Triticale*. Plant Physiol **122:** 687–694

Maron LG, Piñeros MA, Guimarães CT, Magalhaes JV, Pleiman JK, Mao C, Shaff JE, Belicuas SNJ, Kochian LV (2010) Two functionally distinct members of the MATE (multi-drug and toxic compound extrusion) family of transporters potentially underlie two major aluminum tolerance QTLs in maize. Plant J **61:** 728–740

Martínez-Camacho JL, la Vara LG, Hamabata A, Mora-Escobedo R, Calderón-Salinas V (2004) A pH-stating mechanism in isolated wheat (*Triticum aestivum*) aleurone layers involves malic acid transport. J Plant Physiol **161:** 1289–1298

McCormick LH, Borden FY (1972) Phosphate fixation by aluminium in plant roots. Soil Sci Soc Am J **36:** 779–802

Meriga B, Reddy BK, Rao KR, Reddy LA, Kishor PB (2004) Aluminium-induced production of oxygen radicals, lipid peroxidation and DNA damage in seedlings of rice (*Oryza sativa*). J Plant Physiol **161:** 63–68

Meyer S, Mumm P, Imes D, Endler A, Weder B, Al-Rasheid KAS, Geiger D, Marten I, Martinoia E, Hedrich R (2010) AtALMT12 represents an R-type anion channel required for stomatal movement in Arabidopsis guard cells. Plant J **63:** 1054–1062

Pellet DM, Papernik LA, Kochian LV (1996) Multiple aluminum resistance mechanisms in wheat: roles of root apical phosphate and malate exudation. Plant Physiol **112:** 591–597

Piñeros MA, Cançado GMA, Kochian LV (2008a) Novel properties of the wheat aluminum tolerance organic acid transporter (TaALMT1) revealed by electrophysiological characterization in *Xenopus* oocytes: functional and structural implications. Plant Physiol **147:** 2131–2146

Piñeros MA, Cançado GMA, Maron LG, Lyi SM, Menossi M, Kochian LV (2008b) Not all ALMT1-type transporters mediate aluminum-activated organic acid responses: the case of ZmALMT1, an anion-selective transporter. Plant J **53:** 352–367

Ramos-Díaz A, Brito-Argáez L, Munnik T, Hernández-Sotomayor SMT (2007) Aluminum inhibits phosphatidic acid formation by blocking the phospholipase C pathway. Planta **225:** 393–401

Rao IM, Zeigler RS, Vera R, Sarkarung S (1993) Selection and breeding for acid-soil tolerance in crops. Bioscience **43:** 454–465

Rudrappa T, Czymmek KJ, Paré PW, Bais HP (2008) Root-secreted malic acid recruits beneficial soil bacteria. Plant Physiol **148:** 1547–1556

Runge-Metzger A (1995) Closing the cycle: obstacles to efficient P management for improved global security. *In* H Tiessen, ed, Phosphorus in the Global Environment: Transfers, Cycles and Management. John Wiley & Sons, New York, pp 27–42

Ryan PR, Delhaize E, Jones D (2001) Function and mechanism of organic anion exudation from plant roots. Annu Rev Plant Physiol Plant Mol Biol **52:** 527–560

Ryan PR, Shaff JE, Kochian LV (1992) Aluminum toxicity in roots: correlation among ionic currents, ion fluxes, and root elongation in aluminum-sensitive and aluminum-tolerant wheat cultivars. Plant Physiol **99:** 1193–1200

Sas L, Rengel Z, Tang C (2001) Excess cation uptake, and extrusion of protons and organic acid anions by *Lupinus albus* under phosphorus deficiency. Plant Sci **160:** 1191–1198

Sasaki T, Yamamoto Y, Ezaki B, Katsuhara M, Ahn SJ, Ryan PR, Delhaize E, Matsumoto H (2004) A wheat gene encoding an aluminum-activated malate transporter. Plant J **37:** 645–653

Sawaki Y, Iuchi S, Kobayashi Y, Kobayashi Y, Ikka T, Sakurai N, Fujita M, Shinozaki K, Shibata D, Kobayashi M, et al (2009) STOP1 regulates multiple genes that protect Arabidopsis from proton and aluminum toxicities. Plant Physiol **150:** 281–294

Schubert S, Schubert E, Mengel K (1990) Effect of low pH of the root medium on proton release, growth, and nutrient uptake of field beans (*Vicia faba*). Plant Soil **124:** 239–244

Shaff JE, Schultz BA, Craft EJ, Clark RT, Kochian LV (2010) GEOCHEM-EZ: a chemical speciation program with greater power and flexibility. Plant Soil **330:** 207–214

Sivaguru M, Baluška F, Volkmann D, Felle HH, Horst WJ (1999) Impacts of aluminum on the cytoskeleton of the maize root apex: short-term effects on the distal part of the transition zone. Plant Physiol **119:** 1073–1082

Sivaguru M, Fujiwara T, Šamaj J, Baluska F, Yang Z, Osawa H, Maeda T, Mori T, Volkmann D, Matsumoto H (2000) Aluminum-induced 1-3-β-D-glucan inhibits cell-to-cell trafficking of molecules through plasmodesmata: a new mechanism of aluminum toxicity in plants. Plant Physiol **124:** 991–1006

Sun QB, Shen RF, Zhao XQ, Chen RF, Dong XY (2008) Phosphorus enhances Al resistance in Al-resistant *Lespedeza bicolor* but not in Al-sensitive *L. cuneata* under relatively high Al stress. Ann Bot (Lond) **102:** 795–804

Tan K, Keltjens WG (1990a) Interaction between aluminium and phosphorus in sorghum plants. I. Studies with the aluminium sensitive sorghum genotype TAM428. Plant Soil **124:** 15–23

Tan K, Keltjens WG (1990b) Interaction between aluminium and phosphorus in sorghum plants. II. Studies with the aluminium tolerant sorghum genotype SCO283. Plant Soil **124:** 25–32

Tokimasa T, North RA (1996) Effects of barium, lanthanum and gadolinium on endogenous chloride and potassium currents in *Xenopus* oocytes. J Physiol **496:** 677–686

Tzfira T, Tian GW, Lacroix B, Vyas S, Li JX, Leitner-Dagan Y, Krichevsky A, Taylor T, Vainstein A, Citovsky V (2005) pSAT vectors: a modular series of plasmids for autofluorescent protein tagging and expression of multiple genes in plants. Plant Mol Biol **57:** 503–516

Vance CP, Uhde-Stone C, Allan DL (2003) Phosphorus acquisition and use: critical adaptations by plants securing a nonrenewable resource. New Phytol **157:** 423–447

von Uexküll HR, Mutert E (1995) Global extent, development and economic impact of acid soils. Plant Soil **171:** 1–15

Walker TS, Bais HP, Grotewold E, Vivanco JM (2003) Root exudation and rhizosphere biology. Plant Physiol **132:** 44–51

Wilkinson RE, Duncan RR (1989) Sorghum seedling growth as influenced by H^+, Ca^{2+}, and Mn^{2+} concentrations. J Plant Nutr **12:** 1379–1394

Yamaguchi Y, Yamamoto Y, Matsumoto H (1999) Cell death process initiated by a combination of aluminium and iron in suspension cultures of tobacco cells (*Nicotiana tabacum*): apoptosis-like cell death mediated by calcium and proteinase. Soil Sci Plant Nutr **45:** 647–657

Yamaji N, Huang CF, Nagao S, Yano M, Sato Y, Nagamura Y, Ma JF (2009) A zinc finger transcription factor ART1 regulates multiple genes implicated in aluminum tolerance in rice. Plant Cell **21:** 3339–3349

Yan F, Schubert S, Mengel K (1992) Effect of low root medium pH on net proton release, root respiration, and root growth of corn (*Zea mays* L.) and broad bean (*Vicia faba* L.). Plant Physiol **99:** 415–421

Yan X, Lynch JP, Beebe SE (1995) Genetic variation for phosphorus efficiency of common bean in contrasting soil types. I. Vegetative response. Crop Sci **35:** 1086–1093

Yang JL, Zheng SJ, He YF, Matsumoto H (2005) Aluminium resistance requires resistance to acid stress: a case study with spinach that exudes oxalate rapidly when exposed to Al stress. J Exp Bot **56:** 1197–1203

Yoo SD, Cho YH, Sheen J (2007) Arabidopsis mesophyll protoplasts: a versatile cell system for transient gene expression analysis. Nat Protoc **2:** 1565–1572

Zhao J, Fu J, Liao H, Hu MY, Nian H, Hu Y, Qiu L, Dong Y, Yan X (2004) Characterization of root architecture in an applied core collection for phosphorus efficiency of soybean germplasm. Chin Sci Bull **49:** 1611–1620

Zheng SJ, Yang JL, He YF, Yu XH, Zhang L, You JF, Shen RF, Matsumoto H (2005) Immobilization of aluminum with phosphorus in roots is associated with high aluminum resistance in buckwheat. Plant Physiol **138:** 297–303